Self-Regulation of E × B Flow Shear via Plasma Turbulence

N. Vianello,[1] E. Spada,[1] V. Antoni,[1] M. Spolaore,[1] G. Serianni,[1] G. Regnoli,[3]
R. Cavazzana,[1] H. Bergsåker,[2] and J. R. Drake[2]
[1]*Consorzio RFX, Associazione EURATOM-ENEA sulla fusione, C.so Stati Uniti 4, I-35127 Padova (Italy)*
[2]*Alfvén Laboratory, Royal Institute of Technology, Association EURATOM/VR, SE 100 44 Stockholm, Sweden*
[3]*Associazione EURATOM-ENEA sulla fusione, C.R. Frascati, via E. Fermi 45, 00044, Frascati, Italy*
(Received 17 June 2004; published 6 April 2005)

The momentum balance has been applied to the $\mathbf{E} \times \mathbf{B}$ flow in the edge region of a reversed field pinch (RFP) configuration. All terms, including those involving fluctuations, have been measured in stationary condition in the edge region of the Extrap-T2R RFP experiment. It is found that the component of the Reynolds stress driven by electrostatic fluctuations is the term playing the major role in driving the shear of the $\mathbf{E} \times \mathbf{B}$ flow to a value marginal for turbulent suppression, so that the results are in favor of a turbulence self-regulating mechanism underlying the momentum balance at the edge. Balancing the sheared flow driving and damping terms, the plasma viscosity is found anomalous and consistent with the diffusivity due to electrostatic turbulence.

DOI: 10.1103/PhysRevLett.94.135001 PACS numbers: 52.35.Ra, 52.30.–q, 52.55.Lf

Plasma turbulence is a key subject in research for thermonuclear fusion as it is believed to drive the anomalous particle and energy transport [1] which limits the performance of present devices. Research on this field has been fostered by the discovery of regimes of improved confinement, in which turbulent transport is greatly reduced [1] and the setting up of layer of highly sheared plasma flow is observed [2]. This effect has been interpreted as turbulence suppression occurring when the gradient of $\mathbf{E} \times \mathbf{B}$ velocity drift exceeds a critical value related to broadband turbulence frequency and spatial scales [3].

Spontaneous sheared flows due to $\mathbf{E} \times \mathbf{B}$ drift have been observed in the edge region of tokamaks and stellarators, and in some experiments [4], the value of the shear is found close to the ambient turbulence spectrum width, i.e., marginal for turbulence suppression. These features have been proposed to underlay a dynamical link between $\mathbf{E} \times \mathbf{B}$ flows and turbulent transport which eventually leads to a self-regulation process for turbulence [4].

Despite the rich magnetic activity which characterizes this configuration, as far as it concerns the physics of the edge region, the reversed field pinch (RFP) is found to share several features with other magnetic configurations, among which is a particle transport mainly driven by electrostatic turbulence and a highly sheared $\mathbf{E} \times \mathbf{B}$ flow in the direction perpendicular to the local magnetic field (i.e., the toroidal direction in a RFP) with a shear value close to turbulence suppression [5,6]. This Letter is aimed to discuss the momentum balance in the edge region of a RFP configuration, focusing on the dynamical link between fluctuations and $\mathbf{E} \times \mathbf{B}$ sheared flows suggested by the aforementioned features. For this purpose, the momentum balance has been addressed by the equations of motion and continuity for a compressible plasma:

$$mn\left(\frac{\partial}{\partial t} + \mathbf{V}\cdot\nabla\right)\mathbf{V} = -\nabla p + \mu\left[\nabla^2\mathbf{V} + \frac{1}{3}\nabla(\nabla\cdot\mathbf{V})\right] + \mathbf{J}\times\mathbf{B} + \mathbf{F}^{\rm nf} \tag{1}$$

$$\frac{\partial n}{\partial t} + \nabla\cdot(n\mathbf{V}) = \nabla\cdot\Gamma^0, \tag{2}$$

where n, p, and $\mathbf{V}$ are the plasma density, pressure, and velocity, m is the ion mass, μ is the viscosity coefficient, Γ^0 is the neutral influx, and $\mathbf{F}^{\rm nf}$ is the neutral friction force estimated according to Ref. [7]. It is worth noting that the high level of density fluctuations ($\tilde{n}/\bar{n} \gtrsim 50\%$) prevents the plasma to be approximated as incompressible. Multiplying Eq. (2) by $m\mathbf{V}$, summing the two equations, and using Ampere's law $\nabla\times\mathbf{B} = \mu_0\mathbf{J}$, a momentum balance equation is obtained, which in tensorial notation reads:

$$\frac{\partial}{\partial t}(mnV_i) + \partial_k\left(mnV_kV_i - \frac{B_kB_i}{\mu_0}\right) = -\partial_i\left(p + \frac{B^2}{2\mu_0}\right) + 2\mu\,\partial_kS_{ki} + mV_i\partial_k\Gamma_k^0 + F_i^{\rm nf}, \tag{3}$$

where S_{ki} represents the deviatoric rate of strain tensor:

$$S_{ki} = \frac{\partial_kV_i + \partial_iV_k}{2} - \frac{\delta_{ki}}{3}\partial_lV_l. \tag{4}$$

By decomposing the variables (ρ, $\mathbf{V}$, $\mathbf{B}$) into their mean and fluctuating parts ($\mathbf{V} = \overline{\mathbf{V}} + \tilde{\mathbf{v}}$, $\mathbf{B} = \overline{\mathbf{B}} + \tilde{\mathbf{b}}$, $\rho = \overline{\rho} + \tilde{\rho}$) and performing an equation ensemble average [8], the toroidal component of Eq. (3) becomes:

$$\frac{\partial\langle\rho V_\phi\rangle}{\partial t}+\frac{\partial}{\partial r}\left[\overline{\rho}\left\langle\tilde{v}_r\tilde{v}_\phi-\frac{\tilde{b}_r\tilde{b}_\phi}{\overline{\rho}\mu_0}\right\rangle+\langle\tilde{\rho}\tilde{v}_r\rangle\overline{V}_\phi+\langle\tilde{\rho}\tilde{v}_\phi\rangle\overline{V}_r+\langle\tilde{v}_r\tilde{v}_\phi\tilde{\rho}\rangle\right]=-\frac{\partial}{\partial r}\left(\overline{\rho}\overline{V}_r\overline{V}_\phi-\frac{\overline{B}_r\overline{B}_\phi}{\mu_0}\right)+\mu\frac{\partial^2\overline{V}_\phi}{\partial r^2}+m\frac{\partial\overline{\Gamma}_r^0}{\partial r}\overline{V}_\phi+\overline{F}_\phi^{\rm nf}, \quad (5)$$

where $\rho = mn$ is the mass density, toroidal and poloidal symmetry ($\frac{\partial}{\partial\phi}=\frac{\partial}{\partial\theta}=0$) for mean quantities has been assumed, and curvature effects have been neglected as at the edge $1/r \ll \frac{\partial}{\partial r}$. In Eq. (5) it has also been assumed that toroidal and poloidal derivatives of the terms containing fluctuating parts can be neglected, as the experimental correlation length $L_{\rm corr}$ along these two directions is longer than that in the radial one. Indeed, $L_{\rm corr}$ is of the order of 10–15 cm in the toroidal (perpendicular) direction [9] and 1 m in the poloidal (parallel) one, whereas in the radial direction is of the order of few centimeters.

In order to measure all terms involved in Eq. (5), a new probe array which combines electrostatic and magnetic measurements has been developed. The magnetic probes consist of two sets of three-axial nested magnetic coils. The electrostatic probe consists of 17 molybdenum pins, whose 5 central ones are used as five-pin-balanced triple probes [10] whereas the others measure the floating potential. Fluctuating perpendicular velocities have been approximated by $\mathbf{E}\times\mathbf{B}$ drift velocity fluctuations, as according to [3] they are commonly referred as the sole advective flow for fluctuations of density temperature and flow. Moreover, the electric field fluctuations have been approximated by floating potential fluctuations gradient, i.e., neglecting temperature fluctuations as commonly done in other configurations [11,12]. This simplification has been verified to slightly affect the momentum balance due to the weak radial dependence of the neglected terms. Therefore, the probe array permits us to measure simultaneously in the same location the toroidal and radial mean velocity, their radial derivatives, and the fluctuations of velocity and magnetic field. First derivative of terms containing magnetic fluctuations and second derivative of toroidal velocity have been estimated from the radial profiles obtained inserting into the plasma shot by shot the probe array. The measured bandwidth is 700 kHz for the electrostatic signals and above 1 MHz for the magnetic ones (-3 dB cutoff at 1.1 MHz), wide enough to include all frequencies relevant for transport. The probe array has been inserted in the edge region of Extrap-T2R RFP experiment ($R/a = 1.24$ m$/0.183$ m) whose vessel is protected by a set of limiters [13]. The location of the limiter defines a last closed flux surface (LCFS) and a scrape-off layer (SOL) behind it. The data analyzed have been collected during the stationary phase of low current ($\sim$60 kA) low magnetic field ($B(a)\approx B_\theta(a)\approx 60$ mT) hydrogen discharges with electron density on axis $\sim 1.5\times 10^{19}$ m^{-3}. In Fig. 1 the radial profile of the toroidal $\mathbf{E}\times\mathbf{B}$ mean velocity is shown. As previously observed [9], the $\mathbf{E}\times\mathbf{B}$ velocity has a minimum 2 mm behind the limiter, located at 0.183 m. According to Ref. [14] turbulence can be radially decorrelated by $\mathbf{E}\times\mathbf{B}$ velocity shear if the shearing frequency ω_s ($\omega_s = k_\perp \Delta r dV_{\mathbf{E}\times\mathbf{B}}/dr$) is larger than the ambient turbulence spectrum width $\Delta\omega_t$. In the higher shear region right inside the LCFS, given the typical values of $\Delta\omega_t$ ($\sim 2\times 10^6$ rad/s), of the turbulence radial correlation length Δr ($\sim$1 cm), and of the mean toroidal wave vector ($\sim$10 m^{-1}, weighed averaged over the floating potential power spectrum), the resulting $\mathbf{E}\times\mathbf{B}$ velocity shear ($\sim 10^7$ s^{-1}) is found marginal for turbulence decorrelation criteria [14], as reported in [15]. The same marginality is observed in the whole edge region where $k_\perp$ ranges from 10 to 30 m^{-1}. In Fig. 1 the electrostatic particle flux $\Gamma_{\rm es} = \langle\tilde{n}\tilde{v}_r\rangle$ is also shown, confirming that it tends to decrease where the $\mathbf{E}\times\mathbf{B}$ shear increases as noticed in [5].

Experimental results have allowed Eq. (5) to be further simplified as $\overline{B}_r$ vanishes at the edge and all terms containing $\overline{V}_r$, which is of the order of $\sim$20–40 m/s [16], are found to be negligible. Friction with neutrals results small in the region of the inner shear layer [15] and has been also neglected everywhere, though some role close to the wall is expected as discussed in the conclusions. Moreover, previous measurements in Extrap-T2R [9,16] and other RFP [5,6] have shown that in a stationary condition, the neutral influx Γ_r^0 balances most of the particle flux driven by electrostatic turbulence, so that it has been assumed $\Gamma_{\rm es}\approx\Gamma_r^0$ and Eq. (5) becomes:

$$\frac{\partial}{\partial r}\Bigg[\underbrace{\overline{\rho}\left\langle\tilde{v}_r\tilde{v}_\phi-\frac{\tilde{b}_r\tilde{b}_\phi}{\overline{\rho}\mu_0}\right\rangle}_{A}+\underbrace{\langle\tilde{v}_r\tilde{v}_\phi\tilde{\rho}\rangle}_{B}\Bigg]+\underbrace{\Gamma_{\rm es}\frac{\partial\overline{V}_\phi}{\partial r}}_{C}\approx\mu\frac{\partial^2\overline{V}_\phi}{\partial r^2}. \quad (6)$$

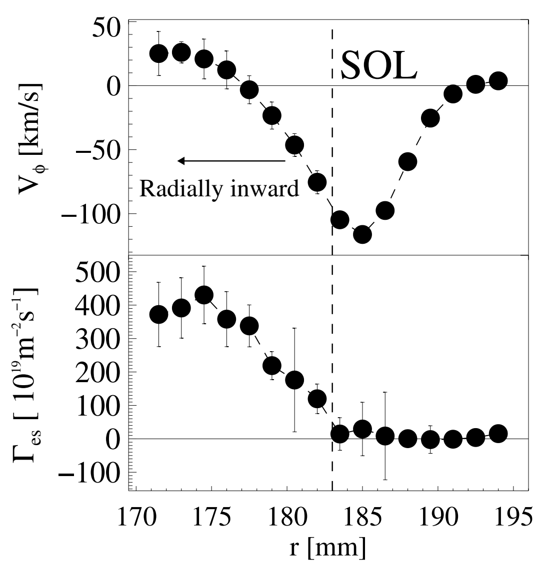

FIG. 1. Radial profile of electrostatic particle flux and of $\mathbf{E}\times\mathbf{B}$ velocity.

Equation (6) shows that in stationary conditions, the viscous force on the right-hand side (RHS) of Eq. (6) equates the three terms driven by plasma fluctuations in the left-hand side (LHS). The probe array has allowed all these terms to be measured and compared with those measured in other configurations. The term A is proportional through the mean mass density to the Reynolds stress tensor defined as $R_{ij} = \langle \tilde{v}_i \tilde{v}_j \rangle - \langle \tilde{b}_i \tilde{b}_j \rangle / \mu_0 \overline{\rho}$. In Fig. 2 the complete Reynolds stress and its electrostatic and magnetic components are shown. The two components have comparable magnitude but different radial behavior: the velocity component increases inside the plasma, while the magnetic one has a less pronounced radial dependence. Therefore, the radial gradient of the Reynolds stress is mainly determined by electrostatic turbulence and to take place where the flow is highly sheared, in analogy to what is observed in stellarators and tokamaks [11,12,17]. Therefore, as in the momentum balance [Eq. (6)] enters the radial derivative of the Reynolds stress, it turns out that in a RFP, despite the high level of magnetic fluctuations, mainly velocity fluctuations contribute to flow generation. The term B, which arises only for a compressible plasma, represents the three wave coupling between fluctuations of density and velocities perpendicular to $\mathbf{B}$ and it is reminiscent of the term entering in energy transfer process from drift-wave-induced turbulence and mean flow [18–20]. In the same Fig. 2, the lower panel shows the radial profile of this term, normalized to the mean mass density in order to compare it directly to the Reynold stress term. It is found negligible everywhere apart in the region across the LCFS where it is comparable to the Reynolds stress, little affecting the momentum balance away from a region close to the wall. It is worth noting that the minimum of the triple term occurs in proximity of the shear layer exactly as observed in a stellarator [18]. In that experiment, the proximity was interpreted as a further indication of $\mathbf{E} \times \mathbf{B}$ flow sustainment by fluctuations.

According to Eq. (6), the radial derivatives of Reynolds stress tensor and of the triple product, and the term C, which represents the rate of momentum exchanged by diffusion in a nonuniform velocity field, can either oppose to or favor the viscous force. To establish their action and relative strength, the three terms in the LHS of Eq. (6) have been compared, in value and sign, in Fig. 3, where the radial derivative of terms A, B, and the term C are compared with the $\mathbf{E} \times \mathbf{B}$ velocity second radial derivative, entering in the viscous dissipation: terms with the same sign of second derivative are identified as terms opposing the viscous force action and vice versa. It appears that at the edge inside the LCFS and in the SOL, all the terms oppose apart the derivative of the triple correlation product for $r \leq 178$ mm. The term proportional to Reynolds stress gradient is the dominant term inside the LCFS, then manifesting a leading role in flow generation. Therefore, as the viscous force tends to smooth the velocity profile, Reynolds stress appears as the term which sustains the shear velocity inside the LCFS. This result allows us to add another analogy with other magnetic configurations, where Reynolds stress has already been suggested to play an important role in flow generation at the edge

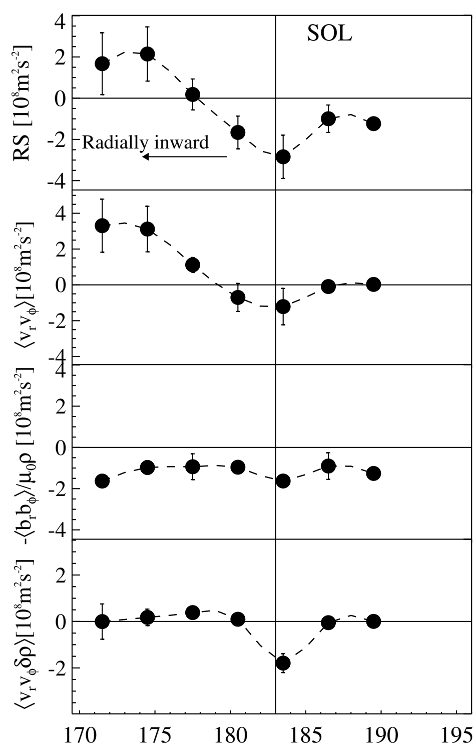

FIG. 2. From top to bottom: radial profiles of complete Reynolds stress tensor, of its electrostatic and magnetic components, of the normalized term $B = \langle \tilde{v}_r \tilde{v}_\phi \tilde{\rho} \rangle = \langle \tilde{v}_r \tilde{v}_\phi \frac{\tilde{\rho}}{\bar{\rho}}$. Dotted lines indicate a spline interpolation.

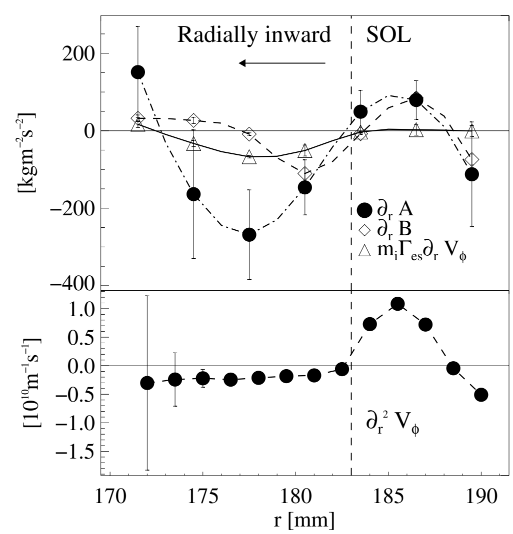

FIG. 3. Radial derivative of terms A (dots), B (diamond), and term C (triangle) of Eq. (6) and second derivative of $\mathbf{E} \times \mathbf{B}$ velocity. Dotted lines in the upper panel show the result of spline interpolation.

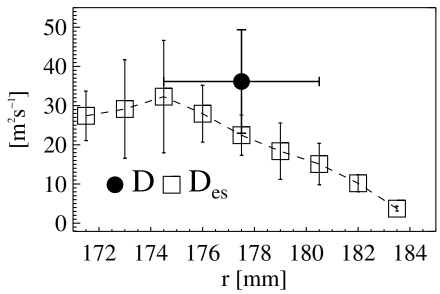

FIG. 4. Average effective diffusion coefficient (black dots) compared with the radial profile of the diffusion coefficient obtained from electrostatic turbulence (open square).

[4,11,18,21–23]. For completeness it should be noted that in the region closer to the LCFS, other terms, here neglected, could play a relevant role in the momentum balance and, namely, the force due to finite Larmor radius (FLR) losses [24], the friction with neutrals and the parallel losses, the latter caused by field lines intercepting the walls which could add an additional damping. The first two terms have been estimated and are found to little affect the momentum balance in the region inside the LCFS where the innermost shear layer takes place: the third one is also expected to little affect the global balance, as in Extrap-T2R during the present campaign, the tearing modes always rotate so that the radial component of magnetic field, as measured by the probes, is low. Therefore, an average perpendicular viscosity can be estimated, in particular, in the region from $r \gtrsim 175$ mm to near the wall. As observed in Fig. 3, the velocity second derivative in the RHS of Eq. (6) changes sign across the LCFS as well as the sum of the three terms of the LHS, so that viscosity can be estimated as the ratio between the spatial averages of the LHS of the equation and of the velocity second derivative itself. In analogy to the collisional case, an average effective kinematic diffusivity may be estimated from $\mu = \rho D$ and the result is shown in Fig. 4. The average value, of the order of 36 $m^2\,s^{-1}$, is at least an order of magnitude larger than the collisional kinematic viscosity [25], but consistent, within the error bars, with the value of the effective diffusivity due to the electrostatic turbulence, defined as $D_{es} = \Gamma_{es}/\nabla n$ and shown in the same figure. Therefore, this result indicates that RFP's viscosity is anomalous and closely related to electrostatic turbulence.

In conclusion, for the first time in a RFP configuration, the main terms entering in the momentum balance have been measured, among which are the complete Reynolds stress and the triple correlation product. The Reynold stress is found to be the main term opposing the action of the viscosity inside the LCFS and then driving the inner shear of the $\mathbf{E} \times \mathbf{B}$ velocity. Despite the high level of magnetic fluctuations, velocity fluctuations have been found to play a major role in this process. The viscosity results anomalous and consistent with anomalous diffusion driven by turbulence. The results support a self-regulation process by which turbulence through Reynolds stress drives the $\mathbf{E} \times \mathbf{B}$ flow shear to a value marginal for suppression of turbulence itself [4], so that the spontaneous $\mathbf{E} \times \mathbf{B}$ flow shear results as a balance of these two competing processes.

The authors wish to thank Rita Lorenzini, R. Paccagnella, and M. Cecconello for valuable discussions.

[1] B. A. Carreras, IEEE Trans. Plasma Sci. **25**, 1281 (1997).
[2] K. Burrell, Phys. Plasmas **6**, 4418 (1999).
[3] P. W. Terry, Rev. Mod. Phys. **72**, 109 (2000).
[4] C. Hidalgo *et al.*, New J. Phys. **4**, 51 (2002).
[5] V. Antoni *et al.*, Phys. Rev. Lett. **80**, 4185 (1998).
[6] V. Antoni, Plasma Phys. Controlled Fusion **39**, B223 (1997).
[7] M. Tendler and D. Heifetz, Fusion Technol. **11**, 289 (1987).
[8] A. Yoshizawa, S.-I. Itoh, K. Itoh, and N. Yokoi, Plasma Phys. Controlled Fusion **46**, R25 (2004).
[9] N. Vianello *et al.*, Plasma Phys. Controlled Fusion **44**, 2513 (2002).
[10] H. Y. W. Tsui *et al.*, Rev. Sci. Instrum. **63**, 4608 (1992).
[11] C. Hidalgo *et al.*, Phys. Rev. Lett. **83**, 2203 (1999).
[12] Y. H. Xu *et al.*, Phys. Rev. Lett. **84**, 3867 (2000).
[13] P. Brunsell *et al.*, Plasma Phys. Controlled Fusion **43**, 1457 (2001).
[14] H. Biglari, P. H. Diamond, and P. W. Terry, Phys. Fluids B **2**, 1 (1990).
[15] G. Serianni *et al.*, Czech. J. Phys. **51**, 1119 (2001).
[16] M. Cecconello, in *Proceedings of the 29th EPS Conference on Plasma Physics and Controlled Fusion, Montreux, 17–21 June 2002*, edited by R. Behn and C. Varandas (European Physical Society, Montreux, Switzerland, 2002), Vol. 26B, Paper P-4.074.
[17] C. Hidalgo *et al.*, Plasma Phys. Controlled Fusion **42**, A153 (2000).
[18] P. H. Diamond *et al.*, Phys. Rev. Lett. **84**, 4842 (2000).
[19] C. Holland *et al.*, Nucl. Fusion **43**, 761 (2003).
[20] M. G. Shats and W. M. Solomon, Phys. Rev. Lett. **88**, 045001 (2002).
[21] P. H. Diamond and Y. B. Kim, Phys. Fluids B **3**, 1626 (1991).
[22] S. B. Korsholm *et al.*, Plasma Phys. Controlled Fusion **43**, 1377 (2001).
[23] A. Hasegawa and M. Wakatani, Phys. Rev. Lett. **59**, 1581 (1987).
[24] V. Antoni *et al.*, Phys. Rev. Lett. **79**, 4814 (1997).
[25] S. I. Braginskii, in *Reviews of Plasma Physics*, edited by M. A. Leontovich, (Consultants Bureau, New York, 1965).